Stable Heating of Cluster Cooling Flows by Cosmic-Ray Streaming

Yutaka Fujita

Department of Earth and Space Science, Graduate School of Science, Osaka University, 1-1 Machikaneyama-cho, Toyonaka, Osaka 560-0043, Japan

fujita@vega.ess.sci.osaka-u.ac.jp

and

Yutaka Ohira

Theory Centre, Institute of Particle and Nuclear Studies, KEK, 1-1 Oho, Tsukuba 305-0801, Japan

ABSTRACT

We study heating of cool cores in galaxy clusters by cosmic-ray (CR) streaming using numerical simulations. In this model, CRs are injected by the central active galactic nucleus (AGN) and move outward with Alfvén waves. The waves are excited by the streaming itself and become non-linear. If magnetic fields are large enough, CRs can prevail in and heat the entire core because of a large Alfvén velocity. We find that the CR streaming can stably heat both high and low temperature clusters for a long time without the assistance of thermal conduction, and it can prevent the development of massive cooling flows. If there is even minor contribution of thermal conduction, the heating can be more stabilized. We discuss the reason of the stability and indicate that the CR pressure is insensitive to the change of intracluster medium (ICM), and that the density dependence of the heating term is similar to that of the radiative cooling.

Subject headings: cooling flows — cosmic rays — galaxies: clusters: general — waves — X-rays: galaxies: clusters

1. Introduction

Clusters of galaxies are filled with hot X-ray gas (intracluster medium; ICM). Although the cooling time of the ICM is larger than the age of the Universe for the most part of a cluster, the core is the exception (Sarazin 1986). Since the cooling time at the core ($\sim 10^8$ yr)

is much smaller than the age of the cluster ($\gtrsim 10^9$ yr), a substantial gas inflow, which was called a "cooling flow", was expected to develop (Fabian 1994, and references therein). However, X-ray spectra taken with *ASCA* and *XMM-Newton* did not detect line emission from intermediate or low temperature gas (e.g. Ikebe et al. 1997; Makishima et al. 2001; Peterson et al. 2001; Tamura et al. 2001; Kaastra et al. 2001; Matsushita et al. 2002). This means that the the cooling rate is much smaller than that previously assumed. *Chandra* observations are also consistent with these results (e.g. McNamara et al. 2000; Johnstone et al. 2002; Ettori et al. 2002; Blanton, Sarazin, & McNamara 2003). These observations show that some heat sources balance with radiative cooling and prevent the development of cooling flows.

Many mechanisms for heat sources of the ICM have been proposed. Thermal conduction from the hot outer layers of clusters is one popular idea (Takahara & Takahara 1979, 1981; Tucker & Rosner 1983). This model may work for clusters with a middle or high temperature if the conductivity is $\sim 30\%$ of the Spitzer one (Zakamska & Narayan 2003). However, the conductivity requires fine-tuning (Bregman & David 1988; Brighenti & Mathews 2003; Soker 2003; Guo & Oh 2008). Moreover, since the Spitzer conductivity significantly decreases for low temperature clusters, thermal conduction may not be able to transfer enough energy. The active galactic nuclei (AGNs) at the cluster centers are also considered as heat sources (e.g. Churazov et al. 2001; Quilis, Bower, & Balogh 2001; Brüggen & Kaiser 2002; Basson & Alexander 2003). In fact, it has been observed that the AGNs disturb the surrounding ICM (e.g. Fabian et al. 2000; McNamara et al. 2000; Blanton et al. 2001; McNamara et al. 2001; Mazzotta et al. 2002; Fujita et al. 2002; Johnstone et al. 2002; Kempner, Sarazin, & 2002; Takizawa et al. 2003; Fujita et al. 2004b). However, it is not clear how the energy generated by the AGN is transfered to the ambient ICM. For example, sound waves observed around the AGNs in some clusters were considered the significant channel for the AGN energy input into the ICM (Fabian et al. 2003; Forman et al. 2005). However, theoretical studies have indicated that the dissipation of the sound waves or weak shocks is too fast to heat an entire cool core and thus the waves cannot stably heat the core (Fujita & Suzuki 2005; Mathews, Faltenbacher, & Brighenti 2006; see also Fujita et al. 2007b).

Cosmic-rays (CRs) may be another channel for the AGN energy input into the ICM (e.g. Tucker & Rosner 1983; Böhringer & Morfill 1988; Rephaeli 1987; Rephaeli & Silk 1995; Colafrancesco, Dar, & De Rújula 2004; Pfrommer et al. 2007; Jubelgas et al. 2008). In particular, CR streaming has been investigated as a way through which the CR energy is transfered to the ICM (Böhringer & Morfill 1988; Loewenstein, Zweibel, & Begelman 1991). In this mechanism, PdV work done by the CRs on an Alfvén wave effectively becomes an energy source of the ICM (see § 2.2). It is to be noted that this mechanism may also be working in supernova remnants (e.g. Völk, Drury, & McKenzie 1984; Berezhko & Ellison 1999). For

clusters of galaxies, the models of Böhringer & Morfill (1988) and Loewenstein et al. (1991) are time-independent. Thus, the models cannot treat the ICM that is not in a steady state. Recently, Guo & Oh (2008) studied non-steady models. They combined CR streaming and thermal conduction as heat sources, and showed that the ICM turns out to be in a steady state, and that a cooling flow is suppressed. In their models, CR streaming and thermal conduction seem to equally contribute to the heating of the ICM (their Figure 6). Since they constructed models for a middle-temperature cluster (A 2199), it is not certain whether the models can be applied to low temperature clusters in which thermal conduction is not effective (see Brighenti & Mathews 2003). Moreover, the conductivity of the ICM may be small even for hot clusters. The existence of cold fronts in some clusters means that at least in some regions in those clusters, the conductivity has to be much smaller than the Spitzer value (Ettori & Fabian 2000). Simultaneous heating by both the central AGN and thermal conduction had been proposed by Ruszkowski & Begelman (2002). In their model, mechanical heating through bubble motion was considered for the AGN heating. Since the advantage of CR streaming over the mechanical heating was not clear in the models of Guo & Oh (2008), it may be useful to study the case where a cool core is heated only by CR streaming.

In this study, we revisit the heating of the ICM by CR streaming. We consider non-steady ICM and investigate whether the CR streaming alone can stably heat the ICM without the assistance of thermal conduction. We emphasize that we do not intend to search models in which the heating is completely balanced with radiative cooling. Since the age of clusters is finite (say $\sim$ 5 Gyr; e.g. Kitayama & Suto 1996), it is sufficient to find solutions that are stable for that time. We treat both high and low temperature clusters. We follow the growth of Alfvén waves, which Guo & Oh (2008) did not consider. We simulate for various parameters in order to find the nature of the CR heating, although our goal is not to compare the results with specific clusters in detail, because supplemental heating mechanisms other than CR streaming (e.g. shock heating) are likely to be effective in real clusters. We consider protons as CRs.

The paper is organized as follows. In § 2, we explain our models for CR streaming and galaxy clusters. In § 3, we present the results for various parameters, and show that the CR heating is fairly stable. In § 4, we discuss the reason of the stability. § 5 is devoted to conclusions.

2. Models

2.1. Basic Equations

For simplicity, we assume that the cluster is spherically symmetric. The flow equations are

$$\frac{\partial \rho}{\partial t} + \frac{1}{r^2}\frac{\partial}{\partial r}(r^2 \rho u) = 0 \,, \tag{1}$$

$$\frac{\partial (\rho u)}{\partial t} + \frac{1}{r^2}\frac{\partial}{\partial r}(r^2 \rho u^2) = -\rho \frac{GM(r)}{r^2} - \frac{\partial}{\partial r}(P_g + P_c + P_B) \,, \tag{2}$$

$$\begin{aligned} \frac{\partial e_g}{\partial t} + \frac{1}{r^2}\frac{\partial}{\partial r}(r^2 u e_g) &= -P_g \frac{1}{r^2}\frac{\partial}{\partial r}(r^2 u) + \frac{1}{r^2}\frac{\partial}{\partial r}\left[r^2 \kappa(T)\frac{\partial T}{\partial r}\right] \\ &\quad -n_e^2 \Lambda(T) + H_{\rm st} + H_{\rm coll} \,, \end{aligned} \tag{3}$$

$$\frac{\partial e_c}{\partial t} + \frac{1}{r^2}\frac{\partial}{\partial r}(r^2 \tilde{u} e_c) = -P_c \frac{1}{r^2}\frac{\partial}{\partial r}(r^2 \tilde{u}) + \frac{1}{r^2}\frac{\partial}{\partial r}\left[r^2 D(\rho)\frac{\partial e_c}{\partial r}\right] - \Gamma_{\rm loss} + \dot{S}_c \,, \tag{4}$$

where ρ is the gas density, u is the gas velocity, P_g is the gas pressure, P_c is the CR pressure, P_B is the magnetic pressure, G is the gravitational constant, $M(r)$ is the gravitational mass within the radius r, $\kappa(T) = f_c \kappa_0 T^{5/2}$ is the coefficient for thermal conduction and T is the temperature, n_e is the electron density, Λ is the cooling function, $H_{\rm st}$ is the heating by CR streaming, $H_{\rm coll}$ is the heating by Coulomb and hadronic collisions, $\tilde{u}$ is the CR transport velocity, $D(\rho)$ is the diffusion coefficient for CRs averaged over the CR spectrum, $\Gamma_{\rm loss}$ is the energy loss by Coulomb and hadronic collisions, and $\dot{S}_c$ is the source term of CRs. Energy densities of the gas and the CRs are respectively defined as $e_g = P_g/(\gamma_g - 1)$ and $e_c = P_c/(\gamma_c - 1)$, where $\gamma_g = 5/3$ and $\gamma_c = 4/3$.

For thermal conductivity, $\kappa_0 = 5 \times 10^{-7}$ in cgs units corresponds to the classical Spitzer value, and f_c is the ratio to that. The cooling function is based on the detailed calculations by Sutherland & Dopita (1993),

$$n_e^2 \Lambda = [C_1 (k_B T)^\alpha + C_2 (k_B T)^\beta + C_3] n_i n_e \,, \tag{5}$$

where n_i is the ion number density and the units for $k_B T$ are keV. For an average metallicity $Z = 0.3\, Z_\odot$ the constants in equation (5) are $\alpha = -1.7$, $\beta = 0.5$, $C_1 = 8.6 \times 10^{-3}$, $C_2 = 5.8 \times 10^{-2}$, and $C_3 = 6.4 \times 10^{-2}$, and we can approximate $n_i n_e = 0.704 (\rho/m_H)^2$. The units of Λ are 10^{-22} ergs cm^3 (Ruszkowski & Begelman 2002). For Coulomb and hadronic collisions, we use $H_{\rm coll} = \eta_c n_e e_c$ and $\Gamma_{\rm loss} = \zeta_c n_e e_c$, where $\eta_c = 2.63 \times 10^{-16}$ cm^3 s^{-1} and $\zeta_c = 7.51 \times 10^{-16}$ cm^3 s^{-1} (Guo & Oh 2008). Since their contributions are minor, the details of the collisions do not affect the results.

2.2. CR Streaming and Heating

Alfvén waves, which scatter CRs, are driven by CR streaming because CRs can give their momentum to the waves through resonance (streaming instability; Skilling 1975; Bell 1978). Since the CRs as a whole move with Alfvén waves, the CR transport velocity in equation (4) is given by $\tilde{u} = u + v_A$, where $v_A = B/\sqrt{4\pi\rho}$ is the Alfvén velocity for a magnetic field B (e.g. Kang & Jones 2006; Guo & Oh 2008; Caprioli, Blasi, & Amato 2009). The wave energy $U_A = \delta B^2/(8\pi)$, where δB is the magnetic field fluctuation, is amplified by the PdV work done by the CRs on Alfvén waves:

$$\frac{\partial U_A}{\partial t} = v_A \left| \frac{\partial P_c}{\partial r} \right| \tag{6}$$

(Lucek & Bell 2000). We solve this equation by setting $U_A = 0$ at $t = 0$.

After the wave energy increases to $U_A \sim U_M$, where $U_M = B^2/(8\pi)$ is the energy of the background magnetic field, the waves are expected to be damped by non-linear effects. Although the exact value of the maximum of U_A has not been known, we set it at U_M. After the wave energy increases to the maximum, the waves are expected to heat ICM (e.g. Ohira et al. 2009; Gargaté et al. 2010). Thus, we give the heating term in equation (3) by

$$H_{\rm st} = \Gamma v_A \left| \frac{\partial P_c}{\partial r} \right| \tag{7}$$

(Völk et al. 1984; Kang & Jones 2006). We expect that $\Gamma \sim 1$ after the wave energy increases to $U_A \sim U_M$. Thus, we simply give $\Gamma = U_A/U_M$ for $U_A < U_M$ and $\Gamma = 1$ after U_A reaches U_M. Since U_A rapidly increases at the cluster core (see § 3.2), the results are not much dependent on the definition of Γ for $U_A < U_M$. Note that Guo & Oh (2008) assumed that Γ is always one.

As the source of CRs, we primarily consider the AGN at the center of the cluster. The CRs may be supplied from bubbles observed in the central region of clusters (Guo & Oh 2008). Moreover, they may also be supplied by strong outbursts of the AGN. In this case, CRs are accelerated at the forward shock of a cocoon and they are distributed in a broad region (Fujita et al. 2007a). In fact, this kind of outbursts have been observed in several clusters (McNamara et al. 2005; Nulsen et al. 2005a,b). Furthermore, cluster mergers generate turbulence around the core (Fujita, Matsumoto, & Wada 2004a; Fujita et al. 2005; Ascasibar & Markevitch 2006), and the turbulence could accelerate and provide CRs in the central region of the clusters (e.g. Ohno, Takizawa, & Shibata 2002; Fujita, Takizawa, & Sarazin 2003; Brunetti et al. 2004; Cassano & Brunetti 2005; Enßlin et al. 2011; Brunetti & Lazarian 2011). Although the supply of the CRs may be intermittent, we study continuous CR injection as the time-average. The source term we adopt is similar to that of Guo & Oh (2008)

and it is simply given by

$$\dot{S}_c = \frac{3-\nu}{4\pi}\frac{L_{\rm AGN}}{r_1^3(r_1/r_0)^{-\nu}-r_0^3}\left(\frac{r}{r_0}\right)^{-\nu}(1-e^{-(r/r_0)^2})e^{-(r/r_1)^2}\,, \tag{8}$$

where $L_{\rm AGN}$ is the energy injection rate from the AGN. This means that CRs are mostly injected at $r_0 \lesssim r \lesssim r_1$. We adopt $r_0 = 20$ kpc following Guo & Oh (2008) based on the observations of bubbles. We also adopt $r_1 = 150$ kpc, which is the size of the radio minihalo observed in the Perseus cluster (Gitti, Brunetti, & Setti 2002). Fujita et al. (2007a) indicated that the ICM might be heated within that radius. The injection rate is $L_{\rm AGN} = \epsilon\dot{M}c^2$, where ϵ is the parameter, $\dot{M}$ is the inflow rate of the gas toward the AGN, and c is the speed of light. Following Guo & Oh (2008), we assume $\nu \sim 3$.

The diffusion of a CR particle depends on its energy, because its resonance with an Alfvén wave depends on the gyro radius. This means that the diffusion coefficient D depends on the energy spectrum of CRs. However, the energy spectrum of CRs ejected from the AGN is unknown. Therefore, we give it as a simple function of the ICM density:

$$D(\rho) = D_0(\rho/\rho_0)^{-d}\,, \tag{9}$$

where D_0 and ρ_0 are respectively the values of D and ρ at $r = 0$ and $t = 0$, and d is the parameter. We included the dependence on ρ, because we expect that the diffusion coefficient is reduced as the ICM is compressed and the magnetic fields are increased (Mathews 2009). We assume that the magnetic fields are $B = B_0(\rho/\rho_0)^d$, where B_0 is the parameter and we take $d = 2/3$.

2.3. Gravitational Matter and Gas Profile

We consider two types of clusters. One is a relatively large cluster and the other is a small cluster. For the profile of the acceleration of gravity or the profile of gravitational matter, we adopt models constructed on observations of the Perseus cluster (large) the Virgo cluster (small).

For the Perseus cluster, Mathews et al. (2006) gave an analytical profile of the acceleration of gravity, $GM(r)/r^2$, which is constructed based on the observations by Churazov et al. (2004). We adopt the profile including the contribution of the central galaxy (§ 2 in Mathews et al. 2006). For the Virgo cluster, we use the density and temperature profiles obtained by Ghizzardi et al. (2004). From their results, we can construct the mass profile assuming that the ICM is almost in pressure equilibrium.

We assume that the ICM is initially isothermal. This is because we do not know the initial distribution of CRs. If we assume that the ICM is isothermal, $u = 0$, and $P_c = 0$ at $t = 0$, the ICM density is relatively low at the cluster center, and $\dot{M}$ is small when t is small. Then, as the ICM cools at the cluster center, $\dot{M}$ and the activity of the central AGN gradually increase, and the CRs injected by the AGN are accumulated in the core. On the other hand, if we adopt the observed current density and temperature profiles, the density at the cluster center is high and the cooling time is small. If we start calculations with $u = 0$ and $P_c = 0$ at $t = 0$, $\dot{M}$ abruptly increases and CRs are injected in a very short time, which causes numerical instability. In reality, it is likely that AGN activities precede cluster formation. Thus, it is natural to assume that some amount of CRs had already been injected when the cool core was established.

At $t = 0$, we assume that the temperature of the large cluster is 7 keV and that of the small cluster is 2.4 keV, which are the values in the outer region of the Perseus and the Virgo cluster, respectively (Churazov et al. 2004; Ghizzardi et al. 2004). The ICM profiles are built so that the ICM is in pressure equilibrium in the given gravitational fields. The normalization of the density is determined so that the density in the outer region of the clusters is identical to the observed ones. The initial velocity of the ICM is $u = 0$. There are no CRs at $t = 0$.

3. Results

3.1. Numerical Methods

The hydrodynamic part of the equations is solved by a second-order advection upstream splitting method (AUSM) based on Liou & Steffen (1993, see also Wada & Norman 2001; Fujita, Suzuki, & Wada 2004c). We use 300 unequally spaced meshes in the radial coordinate to cover a region with a radius of 1 Mpc. The inner boundary is set at $r_{\rm min} = 5$ kpc. We adopt inflow/outflow boundary conditions at the inner and outer radii. Model parameters are presented in Table 1. For gravitational potential, 'P' refers to the Perseus type cluster, and 'V' refers to the Virgo type cluster.

Before we investigate heating by CR streaming. we study a pure cooling flow model for comparison. If there is no heating source ($\epsilon = 0$ and $f_c = 0$; Model LCF0), a cooling flow develops and reaches almost a steady state at $t \gtrsim 4$ Gyr. Figure 1 shows the evolution of $\dot{M}$. At $t = 12$ Gyr, $\dot{M}$ increases to 760 $M_\odot$ yr^{-1}.

3.2. CR Heating

In this subsection, we consider our fiducial model with CR heating (Model LCR0). We did not include thermal conduction or $f_c = 0$. The initial magnetic field and the diffusion coefficient at the cluster center are $B_0 = 10\,\mu$G and $D_0 = 1 \times 10^{26}\,\mathrm{cm^2\,s^{-1}}$, respectively. We use the same value of D_0 for other models including CR heating. The diffusion coefficient is much smaller than the values assumed by Guo & Oh (2008) and Mathews (2009). This is because the Alfvén waves become non-linear ($\delta B \sim B$) as we show bellow. In this case, the diffusion coefficient is close to the one for the Bohm diffusion (equation [14] in Bell 1978) and can be very small. Effectively, the diffusion coefficient we adopted is too small to affect the results. In other words, the results are not much different even if we assume $D_0 = 0$.

Figure 2 shows the profiles of ICM temperature and density for Model LCR0. For $t \gtrsim 4$ Gyr, they do not much change. However, the temperature of the inner boundary $r = r_{\rm min}$ slowly oscillates at $0.6 \lesssim k_B T \lesssim 1$ keV. The oscillation is reflected in $\dot{M}$ (Figure 1). Compared with the pure cooling flow model (Model LCF0), $\dot{M}$ is significantly reduced ($\sim 120\,M_\odot\,\mathrm{yr^{-1}}$ at $t \sim 12$ Gyr), which means that CR streaming can be an effective, stable heating source. Figure 3 shows the evolution of the ratio U_A/U_M. The region where U_A/U_M reaches one expands inward and outward in the cluster. This means that the Alfvén waves become non-linear in a wide region of the cluster at the end of the calculation. It is to be noted that even if we assume $U_A/U_M = 1$ throughout the calculation, the results do not much change. The growth time of U_A is much larger than that for a supernova remnant. The main reason is that the spatial scale of a cluster is much larger than that of the precursor of the shock of a supernova remnant. The difference affects the gradient of P_c in equation (6).

Figure 4 shows the ratios P_c/P_g and P_B/P_g at $t = 9$ Gyr. Both the CR and magnetic pressures are smaller than the gas pressure, although they are relatively large in the central region and cannot be ignored ($P_c/P_g \sim 0.3$ and $P_B/P_g \sim 0.3$). In Figure 5, we show relative importance of the two heating mechanisms ($H_{\rm st}$ and $H_{\rm coll}$) at $t = 9$ Gyr. CR streaming alone can almost balance with radiative cooling except for the very inner region of the cluster. This means that it can heat almost the entire cool core of $r \lesssim 100$ kpc. The contribution of Coulomb and hadronic collisions are minor. Figure 6 shows the evolution of the ratio of the heating by CR streaming to the radiative cooling. The ratio gradually reaches one. The bend at $r \sim 400$ kpc at $t = 6$ Gyr corresponds to the point where U_A reaches U_M (Figure 3).

3.3. Parameter Search

In this subsection, we change model parameters to see how the results are affected by them. Probably, most uncertain parameters in our models are those for the energy input from the AGN. In Models LCRe1 and LCRe2, we change the value of ϵ (Table 1). The evolution of $\dot{M}$ is presented in Figure 7. As is expected, we tend to have a smaller $\dot{M}$ for a larger ϵ. For Model LCRe2, the ICM becomes unstable for $t \gtrsim 8$ Gyr, although $\dot{M}$ is smaller than that in Model LCR0 for a long duration of ~ 5 Gyr ($3 \lesssim t \lesssim 8$ Gyr). The temperature and density profiles are shown in Figure 8. In our source model, CRs are injected most intensively at $r \sim r_0$ (equation [8]). If ϵ is too large, radiative cooling cannot cancel the CR heating at $r \sim r_0$, which makes the temperature and density profiles irregular at $r \sim r_0$. In general, models in which CRs are injected in a too narrow region and/or the ICM is too strongly heated tend to be unstable. Since our simulations are one-dimensional, we cannot investigate what happens after the ICM distribution becomes irregular. Multi-dimensional simulations would be interesting to study that. The instability for Model LCRe2 can be prevented by thermal conduction. Model LCRc is the same as Model LCRe2 but $f_c = 0.1$. In this model, the ICM is stable even at $t \sim 12$ Gyr. Moreover, $\dot{M}$ is smaller than that in Model LCR0 throughout the calculation and $\sim 40\, M_\odot\ \mathrm{yr}^{-1}$ at $t \sim 12$ Gyr (Figure 7). Note that if we do not include heat sources except for the thermal conduction of $f_c = 0.1$, the mass inflow rate is $\dot{M} \sim 400\, M_\odot \mathrm{yr}^{-1}$ at $t \sim 12$ Gyr. This means that the thermal conduction of this level alone cannot effectively halt a cooling flow.

Models LCRn1 and LCRn2 are the cases where the value of ν is changed (Table 1). The evolution of $\dot{M}$ is presented in Figure 9. For a larger ν, CRs are injected more intensively at $r \sim r_0$ (equation [8]). Thus, the ICM becomes unstable at $t \sim 9.6$ Gyr for Model LCRn2. In Model LCRb, we change the strength of the background magnetic fields and adopt $B_0 = 5\mu$G. The results are not much different from those for Model LCR0 ($B_0 = 10\ \mu$G; Figure 9). However, the ICM becomes unstable at $t \sim 10.5$ Gyr.

We also considered a less massive cluster (the Virgo type). The initial ICM temperature (~ 2.4 keV) is much smaller than that of the Perseus type cluster (~ 7 keV). Model SCF0 corresponds to a pure cooling flow. In Figure 10, the mass flow rate amounts to $\dot{M} \gtrsim 80\, M_\odot\ \mathrm{yr}^{-1}$ at the end of the calculation. Model SCR0 includes CR heating. The mass inflow rate is significantly reduced by the heating and $\dot{M} \sim 13\, M_\odot\ \mathrm{yr}^{-1}$ at $t \sim 12$ Gyr (Figure 10). Figure 11 shows the temperature and density distributions for Model SCR0. They are stable until the end of the calculation even if there is no assistance of thermal conduction.

4. Discussion

The above results show that heating by CR streaming can almost balance with radiative cooling, and the heating process is relatively stable, even if there is no thermal conduction. The stability can roughly be explained as follows.

In our calculations, the ICM velocity is much smaller than the Alfvén velocity. Figure 12 is an example (Model LCR0 at $t = 9$ Gyr). This means that v_A is the main contributer of $\tilde{u} = u + v_A$ in equation (4). Owing to the large Alfvén velocity, CRs can prevail in and heat the entire core, which is different from other conventional heating mechanisms such as sound waves or weak shocks (Fujita & Suzuki 2005; Mathews et al. 2006). Moreover, the Alfvén velocity is given by $v_A = B/\sqrt{4\pi\rho} \propto \rho^{d-1/2} \propto \rho^{1/6}$ if we assume $d = 2/3$. Thus, the Alfvén velocity is not much dependent on the ICM. The diffusion term in equation (4) can effectively be ignored because of the small value (§ 3.2). These indicate that the distribution of P_c or e_c is insensitive to the change of local ICM, which makes the CR heating stable. Although the absolute value of P_c increases as $\dot{S}_c (\propto \dot{M})$ increases, the overall shape of the profile of P_c does not much change (Figure 13). Moreover, since P_c reflects accumulation of CRs injected so far, it is insensitive to a temporal change of $\dot{S}_c$.

The stability also resides in the heating function $H_{\rm st} = v_A|\partial P_c/\partial r|$ and its global balance with the radiative cooling function. Here, physical quantities are the typical ones for $\lesssim r$. Since v_A does not much evolve and the overall shape of the profile of P_c does not much change, the heating function can be approximated by $H_{\rm st} \propto \dot{M} f(r)$, where $f(r)$ is a function of r and is almost independent of t. The mass inflow rate is given by $\dot{M} = 4\pi r^2 \rho |u|$, which does not depend on the radius at a given time because of the mass conservation. The flow time of the ICM, $t_{\rm flow} \propto r/|u|$, is nearly proportional to the cooling time of the ICM, $t_{\rm cool} \propto P_g/(n_e^2\Lambda)$, because the flow compensates the cooled gas. Thus, we obtain $H_{\rm st} \propto (\rho^3\Lambda/P_g) r^3 f(r)$. If the ICM is adiabatic. $P_g \propto \rho^{\gamma_g}$, where $\gamma_g = 5/3$. However, radiative cooling is effective in the central region of a cluster, and thus $P_g \propto \rho^{\gamma_g'}$, where $1 < \gamma_g' < 5/3$. Observationally, $\gamma_g' = 1.20 \pm 0.06$ for clusters with a cool core (De Grandi & Molendi 2002). Thus, the heating function $H_{\rm st} (\propto \rho^{3-\gamma_g'}\Lambda)$ is similar to the cooling term ($\propto \rho^2\Lambda$) in equation (3). Because of this, the balance between the heating and the cooling can be maintained.

However, the CR streaming is not perfectly locally stable as was noted by Loewenstein et al. (1991) (see their § 2). Because of this, the ICM becomes unstable at the end of calculations in some models without thermal conduction (e.g. Models LCRe2 and LCRn2). The local instability may be related to emission-line filaments, which may be heated by CRs (Loewenstein et al. 1991). Even so, the ability to keep the ICM stable for a long time makes CR streaming attractive as a heat source of cluster cores. Moreover, the ability makes it easier for the model to attain more stability when it is combined with minor thermal con-

duction (Models LCRc). Weak turbulence may also stabilize the ICM, because it conveys energy as thermal conduction does (Kim & Narayan 2003; Fujita et al. 2004a).

5. Conclusions

We have studied heating of cool cores of galaxy clusters by CR streaming. As the source of CRs, we considered the central AGN in a cluster. The CRs amplify Alfvén waves, with which CRs move outward in the cluster. The ICM is heated through dissipation of the waves.

Using numerical simulations, we found that CR streaming can heat the core for a long time after radiative cooling becomes effective without assistance of thermal conduction. Development of a strong cooling flow is well prevented. CR streaming can effectively heat both high and low temperature clusters. This is because CRs can prevail throughout the core and their distribution is insensitive to the change of the ICM. Thus, the entire core is heated by the CRs. Minor contribution of thermal conduction makes the ICM even more stable.

There are limitations in our simple models. For example, we assumed spherical symmetry of a cluster. In reality, it is likely that CRs are injected anisotropically. Whether this anisotropy is erased or not during the propagation of the CRs in the ICM may depend on the geometry of the magnetic fields on which waves and CRs propagate. Moreover, the CR injection or the acceleration itself is highly uncertain ($\dot{S}_c$ in equation [8]). In the future, γ-ray Observations may reveal CR spectra, which may give us information on CR acceleration in clusters.

We thank the anonymous referee for useful comments. This work was supported by KAKENHI (Y. F.: 20540269, 23540308).

REFERENCES

Ascasibar, Y., & Markevitch, M. 2006, ApJ, 650, 102

Basson, J. F., & Alexander, P. 2003, MNRAS, 339, 353

Bell, A. R. 1978, MNRAS, 182, 147

Berezhko, E. G., & Ellison, D. C. 1999, ApJ, 526, 385

Blanton, E. L., Sarazin, C. L., & McNamara, B. R. 2003, ApJ, 585, 227

Blanton, E. L., Sarazin, C. L., McNamara, B. R., & Wise, M. W. 2001, ApJ, 558, L15

Böhringer, H., & Morfill, G. E. 1988, ApJ, 330, 609

Bregman, J. N., & David, L. P. 1988, ApJ, 326, 639

Brighenti, F., & Mathews, W. G. 2003, ApJ, 587, 580

Brüggen, M., & Kaiser, C. R. 2002, Nature, 418, 301

Brunetti, G., Blasi, P., Cassano, R., & Gabici, S. 2004, MNRAS, 350, 1174

Brunetti, G., & Lazarian, A. 2011, MNRAS, 412, 817

Caprioli, D., Blasi, P., & Amato, E. 2009, MNRAS, 396, 2065

Cassano, R., & Brunetti, G. 2005, MNRAS, 357, 1313

Churazov, E., Brüggen, M., Kaiser, C. R., Böhringer, H., & Forman, W. 2001, ApJ, 554, 261

Churazov, E., Forman, W., Jones, C., Sunyaev, R., Böhringer, H. 2004, MNRAS, 347, 29

Colafrancesco, S., Dar, A., & De Rújula, A. 2004, A&A, 413, 441

De Grandi, S., & Molendi, S. 2002, ApJ, 567, 163

Enßlin, T., Pfrommer, C., Miniati, F., & Subramanian, K. 2011, A&A, 527, A99

Ettori, S., Fabian, A. C., Allen, S. W., & Johnstone, R. M. 2002, MNRAS, 331, 635

Ettori, S., & Fabian, A. C. 2000, MNRAS, 317, L57

Fabian, A. C. 1994, ARA&A, 32, 277

Fabian, A. C. et al. 2000, MNRAS, 318, L65

Fabian, A. C., Sanders, J. S., Allen, S. W., Crawford, C. S., Iwasawa, K., Johnstone, R. M., Schmidt, R. W., & Taylor, G. B. 2003, MNRAS, 344, L43

Forman, W., et al. 2005, ApJ, 635, 894

Fujita, Y., Kohri, K., Yamazaki, R., & Kino, M. 2007a, ApJ, 663, L61

Fujita, Y., Matsumoto, T., & Wada, K. 2004a, ApJ, 612, L9

Fujita, Y., Matsumoto, T., Wada, K., & Furusho, T. 2005, ApJ, 619, L139

Fujita, Y., Takizawa, M., & Sarazin, C. L. 2003, ApJ, 584, 190

Fujita, Y., Sarazin, C. L., Kempner, J. C., Rudnick, L., Slee, O. B., Roy, A. L., Andernach, H., & Ehle, M. 2002, ApJ, 575, 764

Fujita, Y., Sarazin, C. L., Reiprich, T. H., Andernach, H., Ehle, M., Murgia, M., Rudnick, L., & Slee, O. B. 2004b, ApJ, 616, 157

Fujita, Y., & Suzuki, T. K. 2005, ApJ, 630, L1

Fujita, Y., Suzuki, T. K., Kudoh, T., & Yokoyama, T. 2007b, ApJ, 659, L1

Fujita, Y., Suzuki, T. K., & Wada, K. 2004c, ApJ, 600, 650

Gargaté, L., Fonseca, R. A., Niemiec, J., Pohl, M., Bingham, R., & Silva, L. O., 2010, ApJ, 711, L127

Ghizzardi, S., Molendi, S., Pizzolato, F., & De Grandi, S. 2004, ApJ, 609, 638

Gitti, M., Brunetti, G., & Setti, G. 2002, A&A, 386, 456

Guo, F., & Oh, S. P. 2008, MNRAS, 384, 251

Ikebe, Y., et al. 1997, ApJ, 481, 660

Johnstone, R. M., Allen, S. W., Fabian, A. C., & Sanders, J. S. 2002, MNRAS, 336, 299

Jubelgas, M., Springel, V., Enßlin, T., & Pfrommer, C. 2008, A&A, 481, 33

Kaastra, J. S., Ferrigno, C., Tamura, T., Paerels, F. B. S., Peterson, J. R., & Mittaz, J. P. D. 2001, A&A, 365, L99

Kang, H., & Jones, T. W. 2006, Astroparticle Physics, 25, 246

Kempner, J. C., Sarazin, C. L., & Ricker, P. M. 2002, ApJ, 579, 236

Kim, W.-T., & Narayan, R. 2003, ApJ, 596, L139

Kitayama, T., & Suto, Y. 1996, ApJ, 469, 480

Liou, M., & Steffen, C. 1993, J. Comp. Phys., 107, 23

Loewenstein, M., Zweibel, E. G., & Begelman, M. C. 1991, ApJ, 377, 392

Lucek, S. G., & Bell, A. R. 2000, MNRAS, 314, 65

Makishima, K., et al. 2001, PASJ, 53, 401

Mathews, W. G. 2009, ApJ, 695, L49

Mathews, W. G., Faltenbacher, A., & Brighenti, F. 2006, ApJ, 638, 659

Matsushita, K., Belsole, E., Finoguenov, A., Böhringer, H. 2002, A&A, 386, 77

Mazzotta, P., Kaastra, J. S., Paerels, F. B., Ferrigno, C., Colafrancesco, S., Mewe, R., & Forman, W. R. 2002, ApJ, 567, L37

McNamara, B. R., et al. 2000, ApJ, 534, L135

McNamara, B. R. et al. 2001, ApJ, 562, L149

McNamara, B. R., Nulsen, P. E. J., Wise, M. W., Rafferty, D. A., Carilli, C., Sarazin, C. L., & Blanton, E. L. 2005, Nature, 433, 45

Nulsen, P. E. J., McNamara, B. R., Wise, M. W., & David, L. P. 2005, ApJ, 628, 629

Nulsen, P. E. J., Hambrick, D. C., McNamara, B. R., Rafferty, D., Birzan, L., Wise, M. W., & David, L. P. 2005, ApJ, 625, L9

Ohira, Y., Reville, B., Kirk, J. G., & Takahara, F. 2009, ApJ, 698, 445

Ohno, H., Takizawa, M., & Shibata, S. 2002, ApJ, 577, 658

Peterson, J. R., et al. 2001, A&A, 365, L104

Pfrommer, C., Enßlin, T. A., Springel, V., Jubelgas, M., & Dolag, K. 2007, MNRAS, 378, 385

Quilis, V., Bower, R. G., & Balogh, M. L. 2001, MNRAS, 328, 1091

Ruszkowski, M. & Begelman, M. C. 2002, ApJ, 581, 223

Rephaeli, Y. 1987, MNRAS, 225, 851

Rephaeli, Y., & Silk, J. 1995, ApJ, 442, 91

Sarazin, C. L. 1986, Reviews of Modern Physics, 58, 1

Skilling, J. 1975, MNRAS, 173, 255

Soker, N. 2003, MNRAS, 342, 463

Sutherland, R. S. & Dopita, M. A. 1993, ApJS, 88, 253

Takahara, M., & Takahara, F. 1979, Progress of Theoretical Physics, 62, 1253

Takahara, M., & Takahara, F. 1981, Progress of Theoretical Physics, 65, 369

Takizawa, M., Sarazin, C. L., Blanton, E. L., & Taylor, G. B. 2003, ApJ, 595, 142

Tamura, T., et al. 2001, A&A, 365, L87

Tucker, W. H., & Rosner, R. 1983, ApJ, 267, 547

Völk, H. J., Drury, L. O., & McKenzie, J. F. 1984, A&A, 130, 19

Wada, K. & Norman, C. A. 2001, ApJ, 547, 172

Zakamska, N. L., & Narayan, R. 2003, ApJ, 582, 162

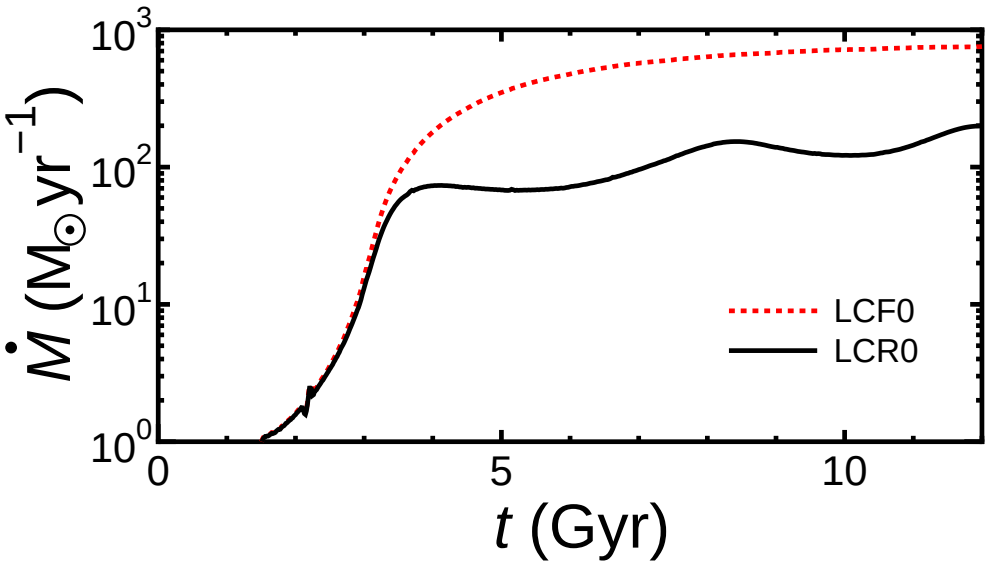

Fig. 1.— Evolution of $\dot{M}$ for Models LCF0, and LCR0

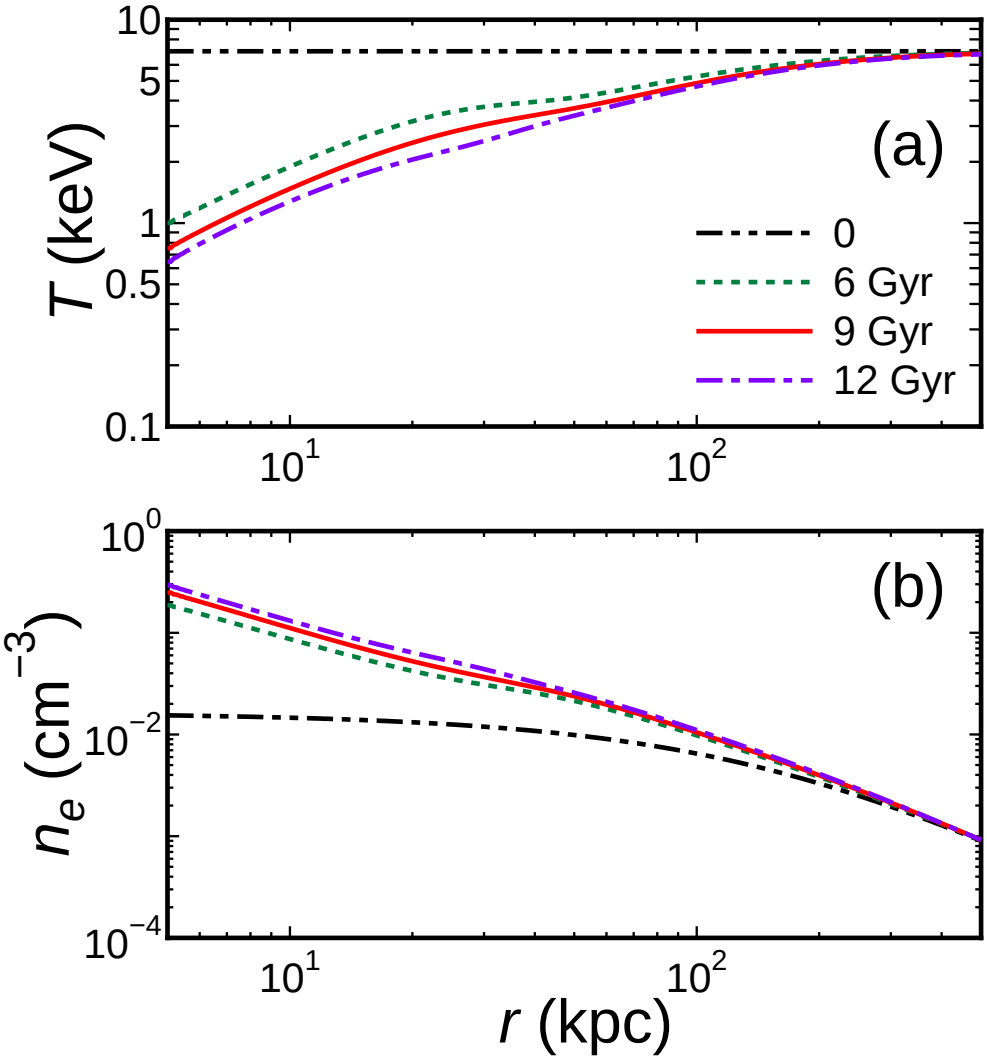

Fig. 2.— (a) Temperature and (b) density profiles for Model LCR0.

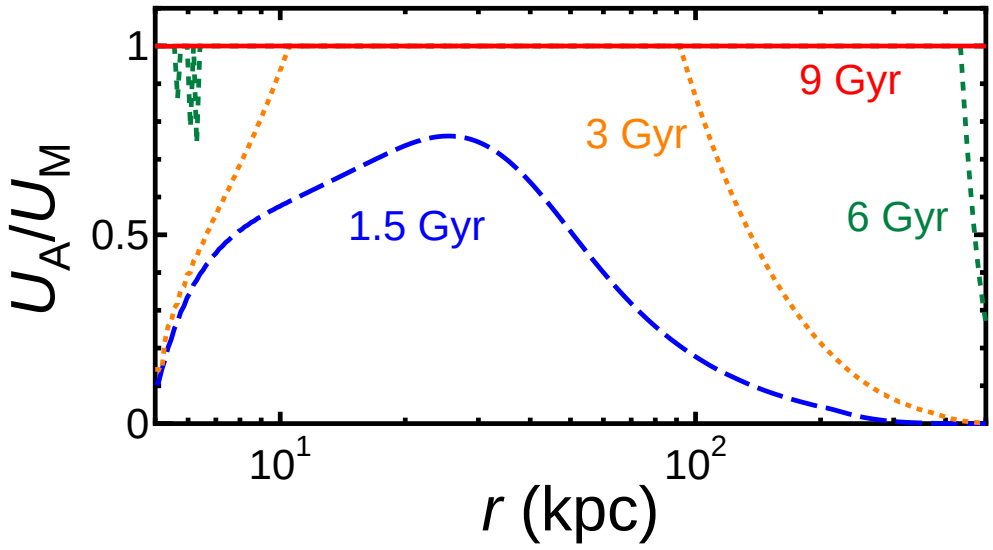

Fig. 3.— Profiles of the ratio U_A/U_M for Model LCR0.

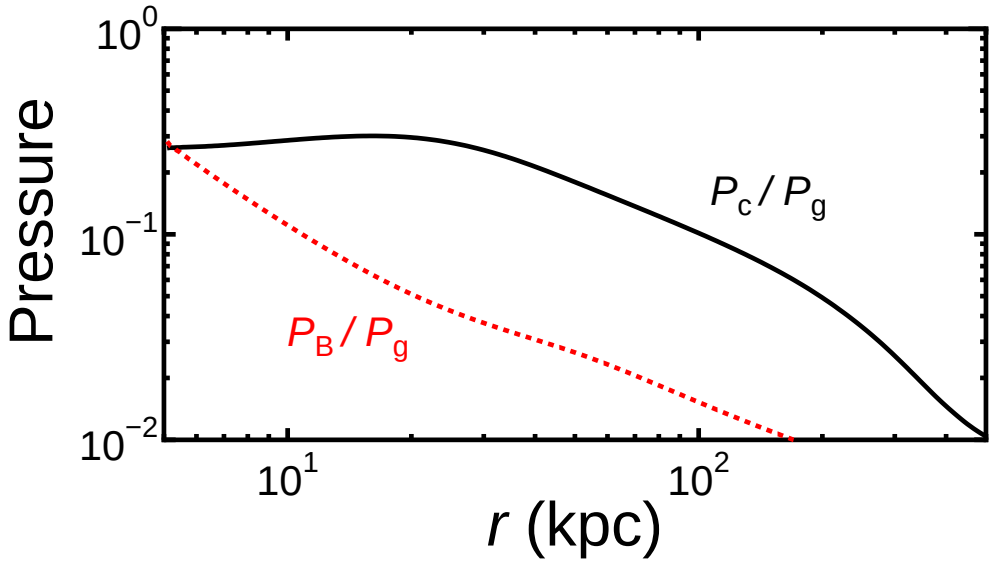

Fig. 4.— Profiles of the ratios P_c/P_g (solid) and P_B/P_g (dotted) at $t = 9$ Gyr for Model LCR0.

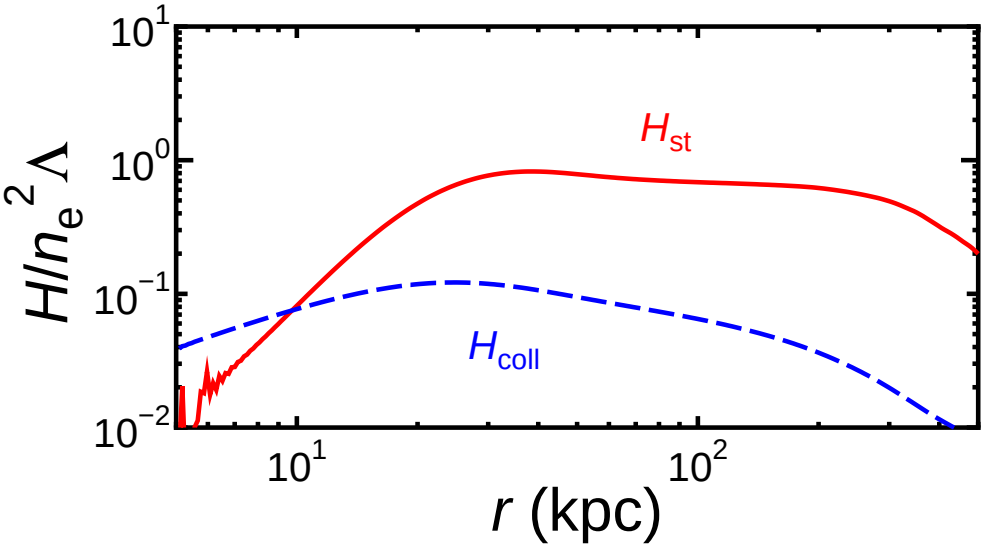

Fig. 5.— Relative importance of CR streaming ($H_{\rm st}$) and collisional heating ($H_{\rm coll}$) at $t =$ 9 Gyr for Model LCR0.

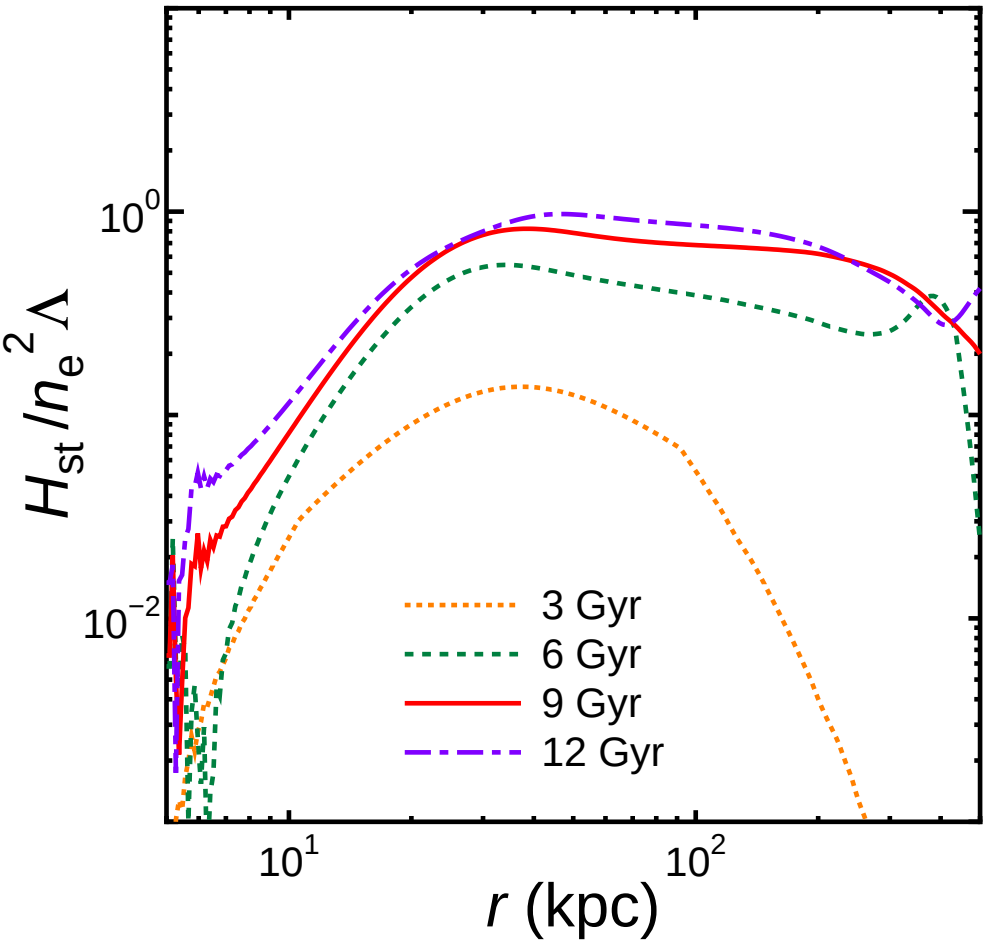

Fig. 6.— Evolution of $H_{\rm st}/(n_e^2\Lambda)$ for Model LCR0.

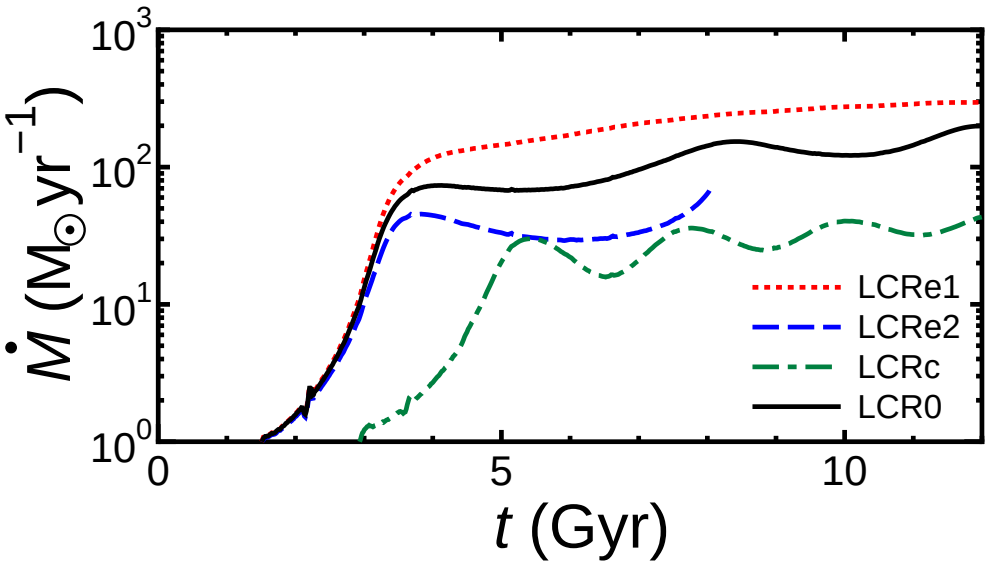

Fig. 7.— The evolution of $\dot{M}$ for Models LCRe1, LCRe2, LCRc, and LCR0.

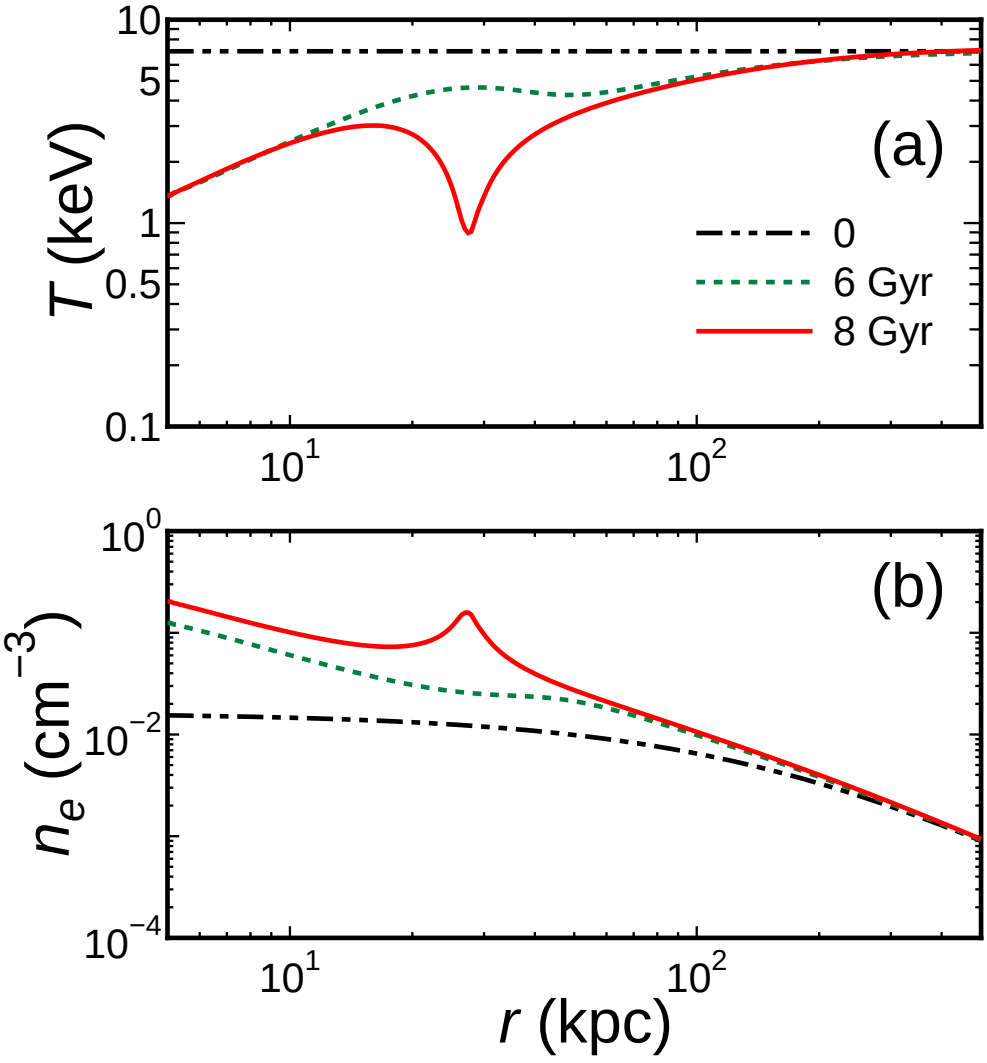

Fig. 8.— (a) Temperature and (b) density profiles for Model LCRe2.

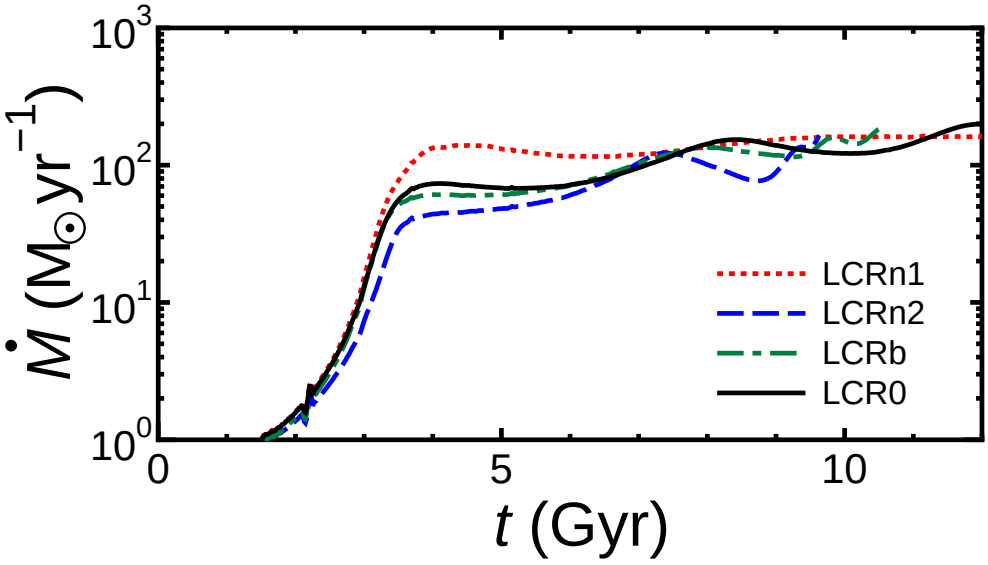

Fig. 9.— Evolution of $\dot{M}$ for Models LCRn1, LCRn2, LCRb, and LCR0.

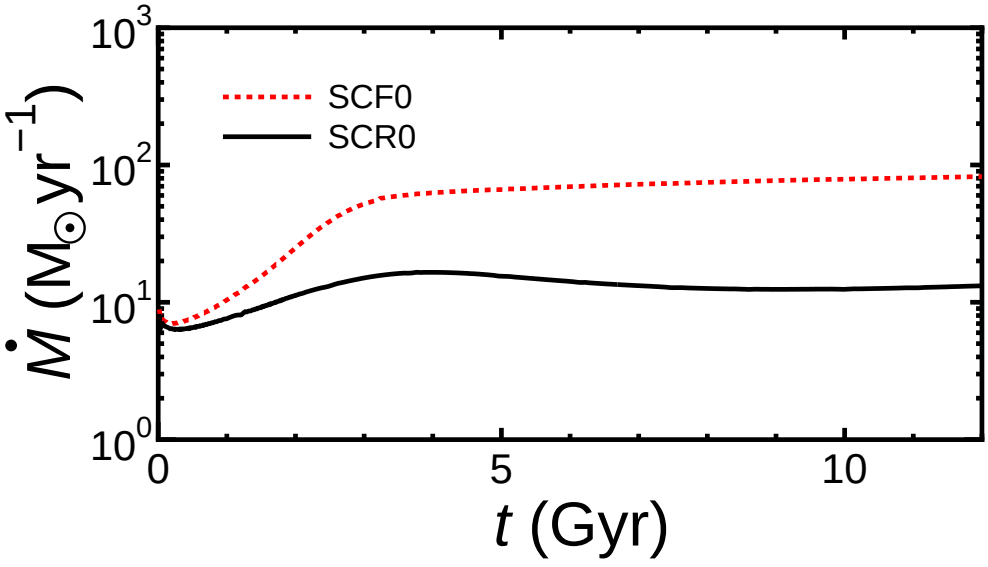

Fig. 10.— Evolution of $\dot{M}$ for Models SCF0, and SCR0

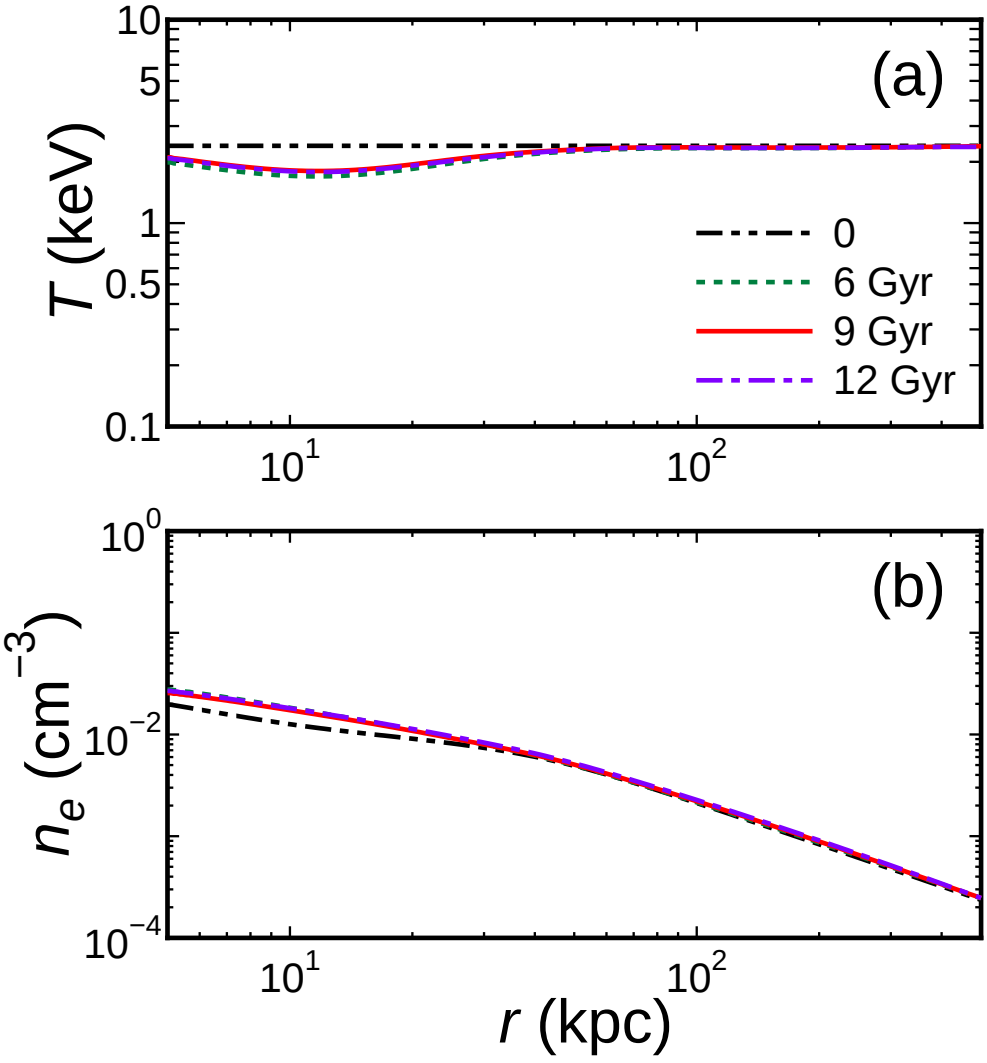

Fig. 11.— (a) Temperature and (b) density profiles for Model SCR0.

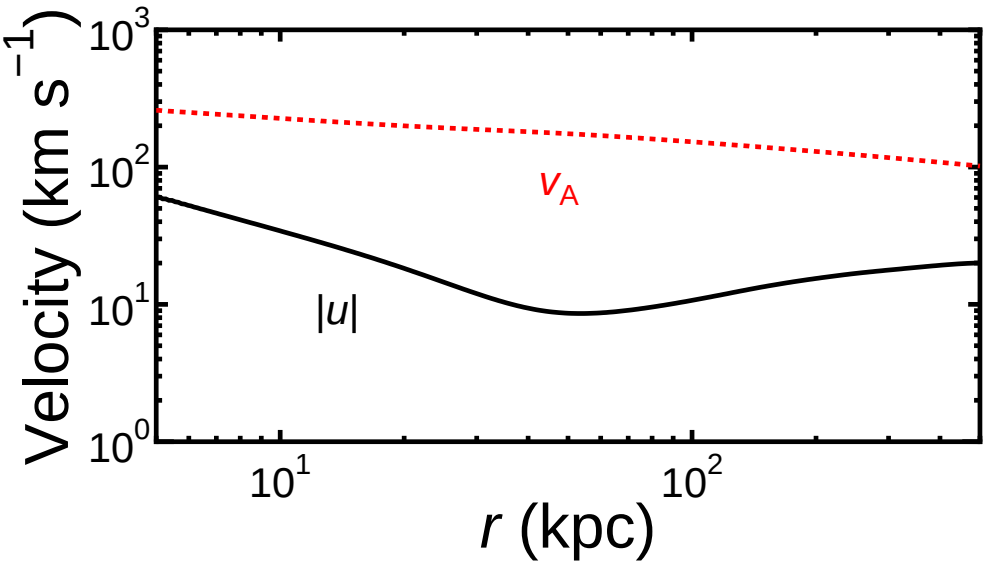

Fig. 12.— ICM velocity and Alfvén velocity profiles at $t = 9$ Gyr for Model LCR0.

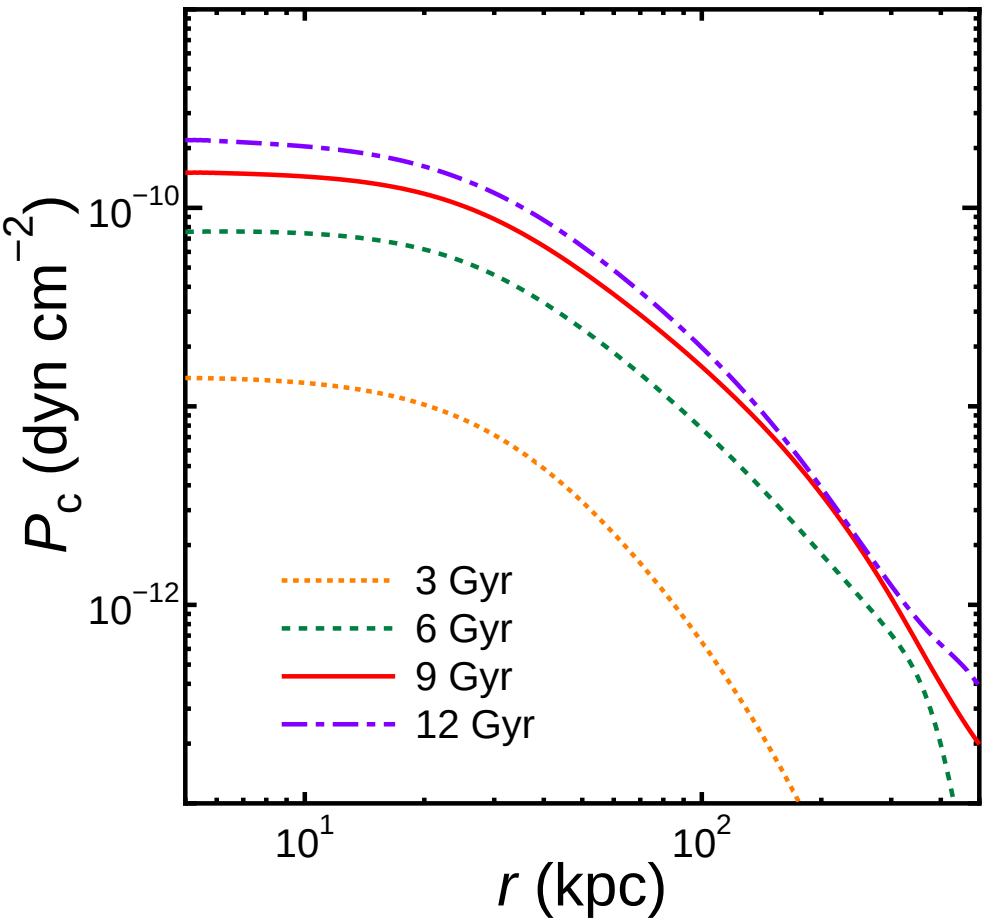

Fig. 13.— CR pressure profiles for Model LCR0.

Table 1. Model Parameters

Model	Potential	B_0 (μG)	f_c	ϵ	ν
LCF0	P	0	0	0	$\cdots$
LCR0	P	10	0	2.5×10^{-4}	3.1
LCRe1	P	10	0	1×10^{-4}	3.1
LCRe2	P	10	0	5×10^{-4}	3.1
LCRc	P	10	0.1	5×10^{-4}	3.1
LCRn1	P	10	0	2.5×10^{-4}	2.5
LCRn2	P	10	0	2.5×10^{-4}	3.5
LCRb	P	5	0	2.5×10^{-4}	3.1
SCF0	V	0	0	0	$\cdots$
SCR0	V	10	0	1×10^{-4}	3.1